Using Fourier series to control mass imperfections in vibratory gyroscopes

Stephan V. Joubert, Hilette Spoelstra and Michael Y. Shatalov

Tshwane University of Technology

July 2014

- In 1890 G.H. Bryan made the following calculation for a body consisting of a ring or cylinder

$$\eta = \frac{\text{Rate of rotation of the vibrating pattern}}{\text{Inertial rate of rotation of the vibrating structure}} \tag{1}$$

is a constant (known today as Bryan's factor) for a fixed mode of vibration.

- Bryan's effect is used to callibrate the resonator gyroscopes (RGs) used navigate, among other craft, the space shuttles and submarines.

- If a disc gyroscope, with known Bryan's factor η, is mounted in a spacecraft and the vibration pattern of the gyroscope is observed, then a slow rate of rotation rate of the craft $\varepsilon\Omega$ may be measured via Formula (1) as

$$\varepsilon\Omega = \frac{\text{Rate of rotation of the vibrating pattern of the gyroscope}}{\eta}. \tag{2}$$

- In 1890 G.H. Bryan made the following calculation for a body consisting of a ring or cylinder

$$\eta = \frac{\text{Rate of rotation of the vibrating pattern}}{\text{Inertial rate of rotation of the vibrating structure}} \tag{1}$$

  is a constant (known today as Bryan's factor) for a fixed mode of vibration.

- Bryan's effect is used to callibrate the resonator gyroscopes (RGs) used navigate, among other craft, the space shuttles and submarines.

- If a disc gyroscope, with known Bryan's factor η, is mounted in a spacecraft and the vibration pattern of the gyroscope is observed, then a slow rate of rotation rate of the craft $\varepsilon\Omega$ may be measured via Formula (1) as

$$\varepsilon\Omega = \frac{\text{Rate of rotation of the vibrating pattern of the gyroscope}}{\eta}. \tag{2}$$

Introduction

- In 1890 G.H. Bryan made the following calculation for a body consisting of a ring or cylinder

$$\eta = \frac{\text{Rate of rotation of the vibrating pattern}}{\text{Inertial rate of rotation of the vibrating structure}} \tag{1}$$

  is a constant (known today as Bryan's factor) for a fixed mode of vibration.

- Bryan's effect is used to callibrate the resonator gyroscopes (RGs) used navigate, among other craft, the space shuttles and submarines.

- If a disc gyroscope, with known Bryan's factor η, is mounted in a spacecraft and the vibration pattern of the gyroscope is observed, then a slow rate of rotation rate of the craft $\varepsilon\Omega$ may be measured via Formula (1) as

$$\varepsilon\Omega = \frac{\text{Rate of rotation of the vibrating pattern of the gyroscope}}{\eta}. \tag{2}$$

Introduction (continued)

- A modern RG:

- An aircraft RG array:

Introduction (continued)

- A modern RG:
  - 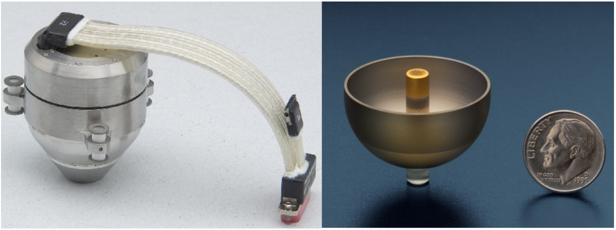

- An aircraft RG array:

Introduction (continued)

- A modern RG:
  - 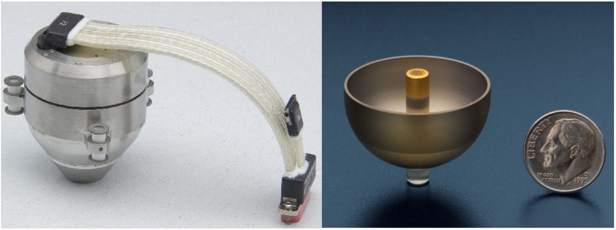

- An aircraft RG array:

Introduction (continued)

- A modern RG:
  -  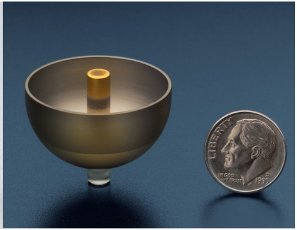

- An aircraft RG array:
  - 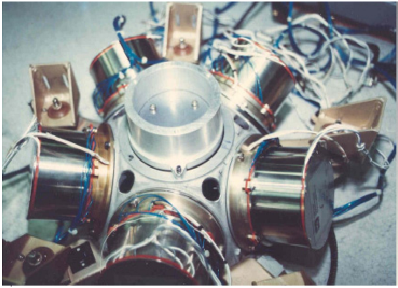 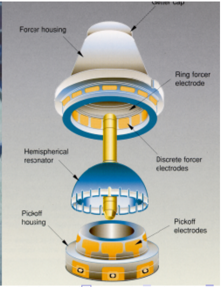

Introduction (continued)

- Bryan's effect may be partially observed in the following photographic experiment of a wineglass filled with milk and excited by a violin bow on the left and, after being placed on a rotating turntable, by a wet finger on the right.

- It is not evident from the photo, but the node does not rotate away from the finger continuously, but is "captured" in a fixed position.

Introduction (continued)

- Bryan's effect may be partially observed in the following photographic experiment of a wineglass filled with milk and excited by a violin bow on the left and, after being placed on a rotating turntable, by a wet finger on the right.

- 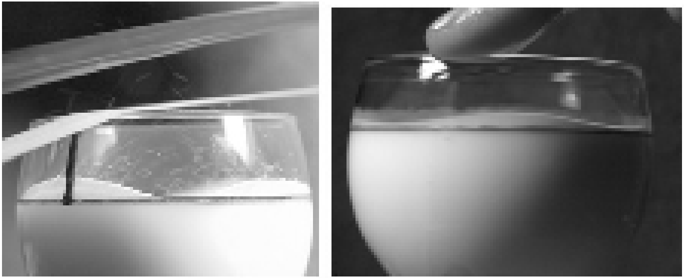

- It is not evident from the photo, but the node does not rotate away from the finger continuously, but is "captured" in a fixed position.

Introduction (continued)

- Bryan’s effect may be partially observed in the following photographic experiment of a wineglass filled with milk and excited by a violin bow on the left and, after being placed on a rotating turntable, by a wet finger on the right.
- 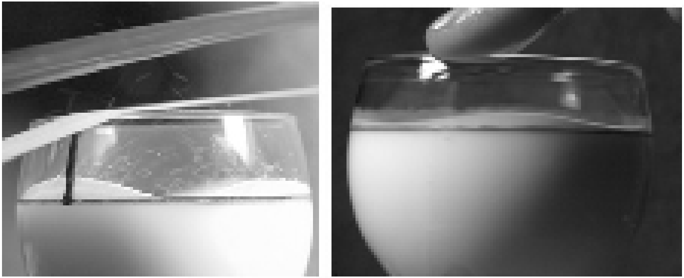
- It is not evident from the photo, but the node does not rotate away from the finger continuously, but is "captured" in a fixed position.

Introduction (continued)

- This "capture effect" is predictable when mass imperfections are introduced into the equations of motion of the body. Indeed this was demonstrated at the TIME 2012 conference by Joubert, Shatalov and Coetzee (see the proceedings of TIME2012 as published in the Journal of Symbolic Computation, 2014).
- Indeed, the TIME2012 paper revealed that for the m^{th} mode of vibration, the precession angle $m\,\Theta$ behaves as demonstrated in the following graph:

Introduction (continued)

- This "capture effect" is predictable when mass imperfections are introduced into the equations of motion of the body. Indeed this was demonstrated at the TIME 2012 conference by Joubert, Shatalov and Coetzee (see the proceedings of TIME2012 as published in the Journal of Symbolic Computation, 2014).
- Indeed, the TIME2012 paper revealed that for the m^{th} mode of vibration, the precession angle $m\,\Theta$ behaves as demonstrated in the following graph:

Introduction (continued)

- This "capture effect" is predictable when mass imperfections are introduced into the equations of motion of the body. Indeed this was demonstrated at the TIME 2012 conference by Joubert, Shatalov and Coetzee (see the proceedings of TIME2012 as published in the Journal of Symbolic Computation, 2014).
- Indeed, the TIME2012 paper revealed that for the m^{th} mode of vibration, the precession angle $m\,\Theta$ behaves as demonstrated in the following graph:

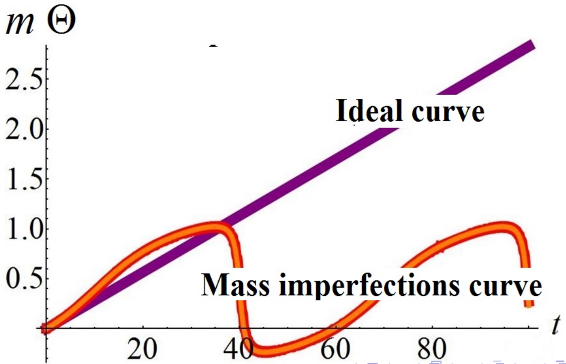

Introduction (continued)

- In this paper we demonstrate how an array of electrodes arranged about a cylindrical disc gyroscope may be modelled by a Fourier series.

- This model shows which electrodes may be manipulated in order to eliminate the influence of the mass imperfections, rendering the gyroscope **"close to the ideal state".**

- In this **"close to the ideal state"** the formula

$$\varepsilon\Omega = \frac{\text{Rate of rotation of the vibrating pattern of the gyroscope}}{\eta}. \tag{3}$$

  is valid, so that Bryan's factor η may be used to navigate a spacecraft by determining the slow rate of rotation $\varepsilon\Omega$.

Introduction (continued)

- In this paper we demonstrate how an array of electrodes arranged about a cylindrical disc gyroscope may be modelled by a Fourier series.

- This model shows which electrodes may be manipulated in order to eliminate the influence of the mass imperfections, rendering the gyroscope **"close to the ideal state".**

- In this **"close to the ideal state"** the formula

$$\varepsilon\Omega = \frac{\text{Rate of rotation of the vibrating pattern of the gyroscope}}{\eta}. \tag{3}$$

is valid, so that Bryan's factor η may be used to navigate a spacecraft by determining the slow rate of rotation $\varepsilon\Omega$.

Introduction (continued)

- In this paper we demonstrate how an array of electrodes arranged about a cylindrical disc gyroscope may be modelled by a Fourier series.

- This model shows which electrodes may be manipulated in order to eliminate the influence of the mass imperfections, rendering the gyroscope **"close to the ideal state".**

- In this **"close to the ideal state"** the formula

$$\varepsilon\Omega = \frac{\text{Rate of rotation of the vibrating pattern of the gyroscope}}{\eta}. \tag{3}$$

  is valid, so that Bryan's factor η may be used to navigate a spacecraft by determining the slow rate of rotation $\varepsilon\Omega$.

Equations of motion of an ideal disc

- Consider the slow rotation rate $\varepsilon\Omega$ of a vibrating cylindrical disc as depicted in the following graph, where P is a particle vibrating in the disc:

Equations of motion of an ideal disc

- Consider the slow rotation rate $\varepsilon\Omega$ of a vibrating cylindrical disc as depicted in the following graph, where P is a particle vibrating in the disc:

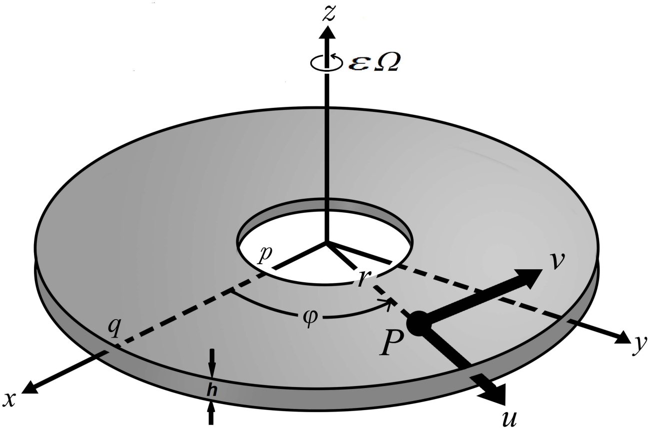

-

Equations of motion of an ideal disc continued

- As explained in the TIME 2012 paper, we assume that the radial displacement u and tangential displacement v of a particle P in the disc can be expressed as:

$$u\left(r,\varphi,t\right) = U(r)\left[C\left(t\right)\cos m\varphi + S\left(t\right)\sin m\varphi\right], \quad (4)$$

$$v\left(r,\varphi,t\right) = V(r)\left[C\left(t\right)\sin m\varphi - S\left(t\right)\cos m\varphi\right]. \quad (5)$$

  Here the integer m is the circumferential wave number, U and V are eigenfunctions (both are combinations of Bessel functions) corresponding to the angular frequency of vibration ω and C and S are functions of time.

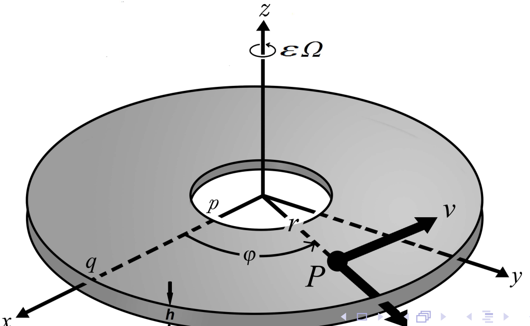

Equations of motion including mass imperfections

- For a disc with mass imperfections that vary circumferentially, the TIME 2012 paper revealed that a Fourier series for the density of the form
$$\rho(\varphi) = \rho_0(1 + 2\varepsilon\frac{I_0}{I_3}(\rho_c \cos 2m\varphi + \rho_s \sin 2m\varphi)) \tag{6}$$
suffices to predict the behaviour of the precession angle.

- Here ε is the dimensionless parameter that is a measure of smallness mentioned above and ρ_0 is the average density of the disc where the dimensionless numbers ρ_c and ρ_s remind us that we are dealing respectively with the coefficient of the cosine and sine components of the $2m^{th}$ harmonics. The constants I_0 and I_3 are definite integrals:
$$I_0 = \rho_0 h \int_p^q [U(r)^2 + V(r)^2] r dr,$$
$$I_3 = \rho_0 h \int_p^q [U^2 - V^2] r dr,$$
where U and V are the eigenfunctions mentioned above.

Equations of motion including mass imperfections

- For a disc with mass imperfections that vary circumferentially, the TIME 2012 paper revealed that a Fourier series for the density of the form

$$\rho(\varphi) = \rho_0\left(1 + 2\varepsilon\frac{I_0}{I_3}(\rho_c \cos 2m\varphi + \rho_s \sin 2m\varphi)\right) \tag{6}$$

  suffices to predict the behaviour of the precession angle.

- Here ε is the dimensionless parameter that is a measure of smallness mentioned above and ρ_0 is the average density of the disc where the dimensionless numbers ρ_c and ρ_s remind us that we are dealing respectively with the coefficient of the cosine and sine components of the $2m^{th}$ harmonics. The constants I_0 and I_3 are definite integrals:

$$I_0 = \rho_0 h \int_p^q [U(r)^2 + V(r)^2] r dr,$$
$$I_3 = \rho_0 h \int_p^q [U^2 - V^2] r dr,$$

  where U and V are the eigenfunctions mentioned above.

Equations of motion including mass imperfections continued

- In the TIME 2014 paper, considering the Lagrangian L (the difference between the kinetic energy E_k and the potential energy E_p of all of the particles in the disc) that is:

$$L = E_k - E_p, \tag{7}$$

we obtained:

$$\begin{aligned} L = {} & \tfrac{\pi}{2} I_0(\dot{C}^2 + \dot{S}^2) + & (8)\\ & \varepsilon \left[\pi I_1 \Omega(\dot{C}S - C\dot{S}) + \tfrac{\pi}{2} I_0 \rho_c(\dot{C}^2 - \dot{S}^2) + \pi I_0 \rho_s \dot{C}\dot{S}\right] - & (9)\\ & \tfrac{\pi}{2} I_2 \left(C^2 + S^2\right). & (10) \end{aligned}$$

- where

$$I_1 = 2\rho_0 h \int_p^q UVr dr, \tag{11}$$

and I_2 is a definite integral involving elastic constants and the eigenfunctions U and V.

Equations of motion including mass imperfections continued

- In the TIME 2014 paper, considering the Lagrangian L (the difference between the kinetic energy E_k and the potential energy E_p of all of the particles in the disc) that is:

$$L = E_k - E_p, \tag{7}$$

we obtained:

$$L = \frac{\pi}{2} I_0(\dot{C}^2 + \dot{S}^2) + \tag{8}$$
$$\varepsilon \left[\pi I_1 \Omega(\dot{C}S - C\dot{S}) + \frac{\pi}{2} I_0 \rho_c(\dot{C}^2 - \dot{S}^2) + \pi I_0 \rho_s \dot{C}\dot{S}\right] - \tag{9}$$
$$\frac{\pi}{2} I_2 \left(C^2 + S^2\right). \tag{10}$$

- where

$$I_1 = 2\rho_0 h \int_p^q UVrdr, \tag{11}$$

and I_2 is a definite integral involving elastic constants and the eigenfunctions U and V.

Equations of motion including mass imperfections continued

- The two applicable Euler-Lagrange Equations of motion are

$$\frac{d}{dt}\left(\frac{\partial L}{\partial \dot{C}}\right) - \left(\frac{\partial L}{\partial C}\right) = 0 \tag{12}$$

and

$$\frac{d}{dt}\left(\frac{\partial L}{\partial \dot{S}}\right) - \left(\frac{\partial L}{\partial S}\right) = 0. \tag{13}$$

- where Bryan's factor η is given by:

$$-1 \le \eta = \frac{I_1}{I_0} \le 1 \tag{15}$$

and the eigenvalue of vibration ω is given by:

$$\omega = \sqrt{\frac{I_2}{I_0}}. \tag{16}$$

Equations of motion including mass imperfections continued

- The two applicable Euler-Lagrange Equations of motion are

$$\frac{d}{dt}\left(\frac{\partial L}{\partial \dot{C}}\right) - \left(\frac{\partial L}{\partial C}\right) = 0 \tag{12}$$

and

$$\frac{d}{dt}\left(\frac{\partial L}{\partial \dot{S}}\right) - \left(\frac{\partial L}{\partial S}\right) = 0. \tag{13}$$

- These equations yield the equations of motion:

$$\begin{pmatrix} \ddot{C} \\ \ddot{S} \end{pmatrix} + \omega^2 \begin{pmatrix} 1-\varepsilon\rho_c & -\varepsilon\rho_s \\ -\varepsilon\rho_s & 1+\varepsilon\rho_c \end{pmatrix} \begin{pmatrix} C \\ S \end{pmatrix} = 2\eta\varepsilon\Omega \begin{pmatrix} -\dot{S} \\ \dot{C} \end{pmatrix}, \tag{14}$$

- where Bryan's factor η is given by:

$$-1 \leq \eta = \frac{I_1}{I_0} \leq 1 \tag{15}$$

and the eigenvalue of vibration ω is given by:

$$\omega = \sqrt{\frac{I_2}{I_0}}. \tag{16}$$

Equations of motion including mass imperfections continued

- The two applicable Euler-Lagrange Equations of motion are

$$\frac{d}{dt}\left(\frac{\partial L}{\partial \dot{C}}\right) - \left(\frac{\partial L}{\partial C}\right) = 0 \tag{12}$$

and

$$\frac{d}{dt}\left(\frac{\partial L}{\partial \dot{S}}\right) - \left(\frac{\partial L}{\partial S}\right) = 0. \tag{13}$$

- These equations yield the equations of motion:

$$\begin{pmatrix} \ddot{C} \\ \ddot{S} \end{pmatrix} + \omega^2 \begin{pmatrix} 1-\varepsilon\rho_c & -\varepsilon\rho_s \\ -\varepsilon\rho_s & 1+\varepsilon\rho_c \end{pmatrix} \begin{pmatrix} C \\ S \end{pmatrix} = 2\eta\varepsilon\Omega \begin{pmatrix} -\dot{S} \\ \dot{C} \end{pmatrix}, \tag{14}$$

- where Bryan's factor η is given by:

$$-1 \leq \eta = \frac{I_1}{I_0} \leq 1 \tag{15}$$

and the eigenvalue of vibration ω is given by:

$$\omega = \sqrt{\frac{I_2}{I_0}}. \tag{16}$$

Frequency splitting

- The eigenvalues

$$\omega^2\left(1+\varepsilon\sqrt{\rho_c^2+\rho_s^2}\right);\omega^2\left(1-\varepsilon\sqrt{\rho_c^2+\rho_s^2}\right) \tag{17}$$

  of the matrix $\omega^2\begin{pmatrix}1-\varepsilon\rho_c & -\varepsilon\rho_s\\ -\varepsilon\rho_s & 1+\varepsilon\rho_c\end{pmatrix}$ indicate that there "beats" or a frequency splitting present.

- The frequency of the beats is (neglecting $O(\varepsilon^2)$)

$$f=\frac{\varepsilon\omega\sqrt{\rho_c^2+\rho_s^2}}{2\pi}. \tag{18}$$

- This frequency splitting causes the vibratory gyroscope to deviate from ideal behaviour where Bryan's factor can be used for navigation purposes.

Frequency splitting

- The eigenvalues

$$\omega^2 \left(1 + \varepsilon\sqrt{\rho_c^2 + \rho_s^2}\right); \omega^2 \left(1 - \varepsilon\sqrt{\rho_c^2 + \rho_s^2}\right) \tag{17}$$

of the matrix $\omega^2 \begin{pmatrix} 1 - \varepsilon\rho_c & -\varepsilon\rho_s \\ -\varepsilon\rho_s & 1 + \varepsilon\rho_c \end{pmatrix}$ indicate that there "beats" or a frequency splitting present.

- The frequency of the beats is (neglecting $O(\varepsilon^2)$)

$$f = \frac{\varepsilon\omega\sqrt{\rho_c^2 + \rho_s^2}}{2\pi}. \tag{18}$$

- This frequency splitting causes the vibratory gyroscope to deviate from ideal behaviour where Bryan's factor can be used for navigation purposes.

Frequency splitting

- The eigenvalues

$$\omega^2\left(1+\varepsilon\sqrt{\rho_c^2+\rho_s^2}\right);\omega^2\left(1-\varepsilon\sqrt{\rho_c^2+\rho_s^2}\right) \tag{17}$$

of the matrix $\omega^2\begin{pmatrix}1-\varepsilon\rho_c & -\varepsilon\rho_s\\ -\varepsilon\rho_s & 1+\varepsilon\rho_c\end{pmatrix}$ indicate that there "beats" or a frequency splitting present.

- The frequency of the beats is (neglecting $O(\varepsilon^2)$)

$$f=\frac{\varepsilon\omega\sqrt{\rho_c^2+\rho_s^2}}{2\pi}. \tag{18}$$

- This frequency splitting causes the vibratory gyroscope to deviate from ideal behaviour where Bryan's factor can be used for navigation purposes.

Electrode array

- Observe a cylindrical disc of thickness h surrounded by an array of electronic plates each at a small distance d from the cylindrical surface of the disc. These plates, together with the surface of the cylindrical surface of the disc, approximate a "parallel plate capasitor" array:

- Assume that the polar axis runs from the centre of the disc through the centre of the first electrode (using the numbering in the figure) and that the "angular length" of each parallel plate is $2\Delta\varphi$.

Electrode array

- Observe a cylindrical disc of thickness h surrounded by an array of electronic plates each at a small distance d from the cylindrical surface of the disc. These plates, together with the surface of the cylindrical surface of the disc, approximate a "parallel plate capasitor" array:

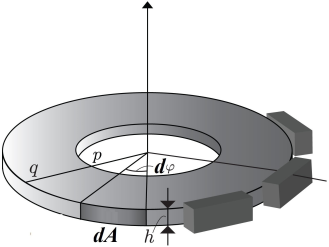

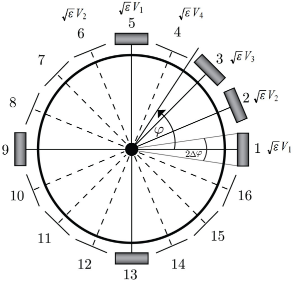

- Assume that the polar axis runs from the centre of the disc through the centre of the first electrode (using the numbering in the figure) and that the "angular length" of each parallel plate is $2\Delta\varphi$.

Electrode array

- Observe a cylindrical disc of thickness h surrounded by an array of electronic plates each at a small distance d from the cylindrical surface of the disc. These plates, together with the surface of the cylindrical surface of the disc, approximate a "parallel plate capasitor" array:

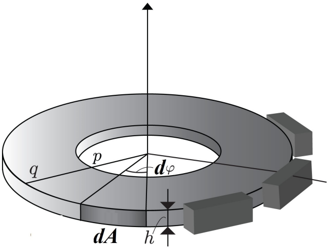

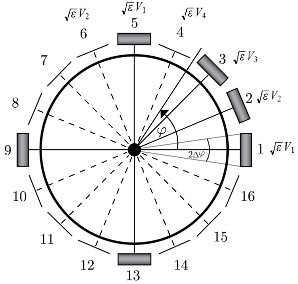

-

- Assume that the polar axis runs from the centre of the disc through the centre of the first electrode (using the numbering in the figure) and that the "angular length" of each parallel plate is $2\Delta\varphi$.

Total electrical potential energy

- Assume that small potential differences $\sqrt{\varepsilon}V_1$, $\sqrt{\varepsilon}V_2$, $\sqrt{\varepsilon}V_3$ and $\sqrt{\varepsilon}V_4$ are maintained between the plate and the disc for capacitors numbered one to four respectively, where we use the small parameter ε again to emphasise smallness.
- Assume that the other potential difference around the disc are $\frac{\pi}{2}$ periodic in the sense that capacitor number five has potential difference $\sqrt{\varepsilon}V_1$, capacitor number six has potential difference $\sqrt{\varepsilon}V_2$, et cetera.

Total electrical potential energy

- Assume that small potential differences $\sqrt{\varepsilon}V_1$, $\sqrt{\varepsilon}V_2$, $\sqrt{\varepsilon}V_3$ and $\sqrt{\varepsilon}V_4$ are maintained between the plate and the disc for capacitors numbered one to four respectively, where we use the small parameter ε again to emphasise smallness.

- Assume that the other potential difference around the disc are $\frac{\pi}{2}$ periodic in the sense that capacitor number five has potential difference $\sqrt{\varepsilon}V_1$, capacitor number six has potential difference $\sqrt{\varepsilon}V_2$, et cetera.

Total electrical potential energy

- Assume that small potential differences $\sqrt{\varepsilon}V_1$, $\sqrt{\varepsilon}V_2$, $\sqrt{\varepsilon}V_3$ and $\sqrt{\varepsilon}V_4$ are maintained between the plate and the disc for capacitors numbered one to four respectively, where we use the small parameter ε again to emphasise smallness.
- Assume that the other potential difference around the disc are $\frac{\pi}{2}$ periodic in the sense that capacitor number five has potential difference $\sqrt{\varepsilon}V_1$, capacitor number six has potential difference $\sqrt{\varepsilon}V_2$, et cetera.
- Now consider a small surface area $dA = h\ q\ d\varphi$ on the cylindrical surface of the disc as depicted in the sketch:

Total electrical potential energy

- Assume that small potential differences $\sqrt{\varepsilon}V_1$, $\sqrt{\varepsilon}V_2$, $\sqrt{\varepsilon}V_3$ and $\sqrt{\varepsilon}V_4$ are maintained between the plate and the disc for capacitors numbered one to four respectively, where we use the small parameter ε again to emphasise smallness.
- Assume that the other potential difference around the disc are $\frac{\pi}{2}$ periodic in the sense that capacitor number five has potential difference $\sqrt{\varepsilon}V_1$, capacitor number six has potential difference $\sqrt{\varepsilon}V_2$, et cetera.
- Now consider a small surface area $dA = h\ q\ d\varphi$ on the cylindrical surface of the disc as depicted in the sketch:

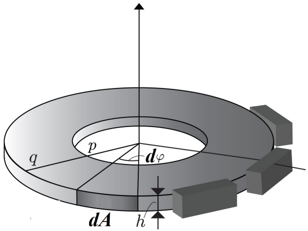

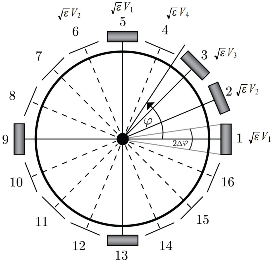

-

Total electrical potential energy continued

- If there is part of a plate covering dA then this *"infinitesimal parallel plate capacitor"* has infinitesimal capacitance

$$dC = \frac{\epsilon_0}{d - u_q} dA = \frac{\epsilon_0 hq}{d - u_q} d\varphi \tag{19}$$

where $\epsilon_0 \approx 8.854 \times 10^{-12}\,\mathrm{F\,.\,m^{-1}}$ is the electromagnetic permittivity of vacuum, d is the gap between the non-vibrating disc and the plate and $u_q = u(q, \varphi, t)$ is the radial displacement of a vibrating particle at the edge of the disc where $r = q$.

- If this *infinitesimal parallel plate capacitor* has a potential difference $\sqrt{\varepsilon} V(\varphi) \neq 0$, then the infinitesimal *electrical potential energy* dE_e stored by the infinitesimal capacitor is

$$dE_e = \frac{\varepsilon V^2(\varphi)}{2} dC = \frac{\epsilon_0 hq}{2\left(d - u_q\right)} \varepsilon V^2(\varphi) d\varphi \tag{20}$$

If there is no part of a plate covering dA then capacitance is zero and there is no potential difference. If we declare $\sqrt{\varepsilon} V(\varphi) = 0$ for this inifinitesimal area, then Equation (20) is still valid.

- If there is part of a plate covering dA then this *"infinitesimal parallel plate capacitor"* has infinitesimal capacitance

$$dC = \frac{\epsilon_0}{d - u_q} dA = \frac{\epsilon_0 hq}{d - u_q} d\varphi \tag{19}$$

where $\epsilon_0 \approx 8.854 \times 10^{-12}\,\mathrm{F\,.\,m^{-1}}$ is the electromagnetic permittivity of vacuum, d is the gap between the non-vibrating disc and the plate and $u_q = u(q, \varphi, t)$ is the radial displacement of a vibrating particle at the edge of the disc where $r = q$.

- If this *infinitesimal parallel plate capacitor* has a potential difference $\sqrt{\varepsilon}V(\varphi) \neq 0$, then the infinitesimal *electrical potential energy* dE_e stored by the infinitesimal capacitor is

$$dE_e = \frac{\varepsilon V^2(\varphi)}{2} dC = \frac{\epsilon_0 hq}{2\,(d - u_q)} \varepsilon V^2(\varphi) d\varphi \tag{20}$$

If there is no part of a plate covering dA then capacitance is zero and there is no potential difference. If we declare $\sqrt{\varepsilon}V(\varphi) = 0$ for this inifinitesimal area, then Equation (20) is still valid.

Total electrical potential energy continued

- Equation (20) may be manipulated as follows:

$$dE_e = \frac{\epsilon_0 hq}{2d}\varepsilon V^2(\varphi)\frac{1}{(1-\frac{u_q}{d})}d\varphi$$
$$= \frac{\epsilon_0 hq}{2d}\varepsilon V^2(\varphi)\left[1+\frac{u_q}{d}+\frac{u_q^2}{d^2}\right]d\varphi \tag{21}$$

because $u_q << d$.

Total electrical potential energy continued

- Equation (20) may be manipulated as follows:

$$dE_e = \frac{\epsilon_0 hq}{2d}\varepsilon V^2(\varphi)\frac{1}{(1-\frac{u_q}{d})}d\varphi$$
$$= \frac{\epsilon_0 hq}{2d}\varepsilon V^2(\varphi)\left[1+\frac{u_q}{d}+\frac{u_q^2}{d^2}\right]d\varphi \quad (21)$$

  because $u_q << d$.

- As stated above, $\varepsilon V^2(\varphi) = 0$ if there is no part of a plate covering the area dA while $\varepsilon V^2(\varphi) = \varepsilon V_1^2$ if dA is covered by the 1^{st}, 5^{th} , 9^{th} or 13^{th} plate, et cetera. An example of the situation is depicted in the following figure:

Total electrical potential energy continued

- Equation (20) may be manipulated as follows:

$$dE_e = \frac{\epsilon_0 hq}{2d}\varepsilon V^2(\varphi)\frac{1}{(1-\frac{u_q}{d})}d\varphi$$
$$= \frac{\epsilon_0 hq}{2d}\varepsilon V^2(\varphi)\left[1+\frac{u_q}{d}+\frac{u_q^2}{d^2}\right]d\varphi \quad (21)$$

because $u_q << d$.

- As stated above, $\varepsilon V^2(\varphi) = 0$ if there is no part of a plate covering the area dA while $\varepsilon V^2(\varphi) = \varepsilon V_1^2$ if dA is covered by the 1^{st}, 5^{th} , 9^{th} or 13^{th} plate, et cetera. An example of the situation is depicted in the following figure:

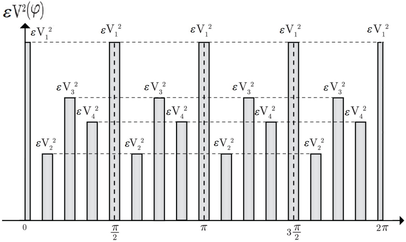

Total electrical potential energy continued

- The total electrical potential is

$$E_e = \frac{\epsilon_0 hq}{2d} \int_0^{2\pi} \varepsilon V^2(\varphi) \left[1 + \frac{u_q}{d} + \frac{u_q^2}{d^2} \right] d\varphi. \tag{22}$$

Total electrical potential energy continued

- The total electrical potential is

$$E_e = \frac{\epsilon_0 hq}{2d} \int_0^{2\pi} \varepsilon V^2(\varphi) \left[1 + \frac{u_q}{d} + \frac{u_q^2}{d^2} \right] d\varphi. \tag{22}$$

- Because of the periodicity involved with the potentials, we may determine a Fourier series for the function $V^2(\varphi)$ depicted in the figure as follows

$$V^2(\varphi) = \frac{a_0}{2} + \sum_{n=1}^{\infty} \left(a_n \cos n\varphi + b_n \sin n\varphi \right) \tag{23}$$

Total electrical potential energy continued

- The total electrical potential is

$$E_e = \frac{\epsilon_0 hq}{2d} \int_0^{2\pi} \varepsilon V^2(\varphi) \left[1 + \frac{u_q}{d} + \frac{u_q^2}{d^2} \right] d\varphi. \qquad (22)$$

- Because of the periodicity involved with the potentials, we may determine a Fourier series for the function $V^2(\varphi)$ depicted in the figure as follows

$$V^2(\varphi) = \frac{a_0}{2} + \sum_{n=1}^{\infty} (a_n \cos n\varphi + b_n \sin n\varphi) \qquad (23)$$

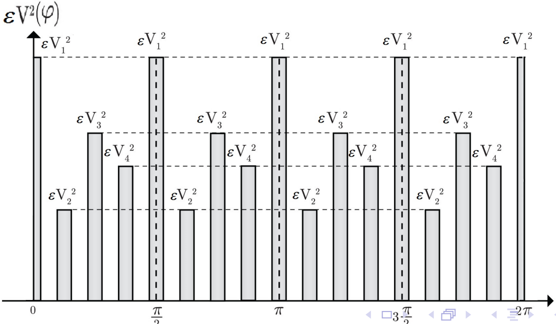

Fourier series for $V^2(\varphi)$

- 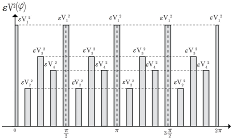

- $$V^2(\varphi) = \frac{a_0}{2} + \sum_{n=1}^{\infty} \left(a_n \cos n\varphi + b_n \sin n\varphi \right) \tag{24}$$

- where

$$a_n = \frac{1}{\pi} \left\{ \int_0^{\Delta\varphi} V_1^2 \cos n\varphi d\varphi + \int_{\frac{\pi}{8}-\Delta\varphi}^{\frac{\pi}{8}+\Delta\varphi} V_2^2 \cos n\varphi d\varphi + \right.$$

$$\int_{\frac{\pi}{4}-\Delta\varphi}^{\frac{\pi}{4}+\Delta\varphi} V_3^2 \cos n\varphi d\varphi + \int_{\frac{3\pi}{8}-\Delta\varphi}^{\frac{3\pi}{8}+\Delta\varphi} V_4^2 \cos n\varphi d\varphi + \tag{25}$$

$$\int_{\frac{\pi}{2}-\Delta\varphi}^{\frac{\pi}{2}+\Delta\varphi} V_1^2 \cos n\varphi d\varphi + \int_{\frac{5\pi}{8}-\Delta\varphi}^{\frac{5\pi}{8}+\Delta\varphi} V_2^2 \cos n\varphi d\varphi + \tag{26}$$

$$\left. \cdots + \int_{2\pi-\Delta\varphi}^{2\pi} V_1^2 \cos n\varphi d\varphi \right\}, \quad n = 0, 1, 2 \cdots . \tag{27}$$

Fourier series for $V^2(\varphi)$

- 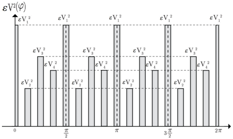

- $$V^2(\varphi) = \frac{a_0}{2} + \sum_{n=1}^{\infty} (a_n \cos n\varphi + b_n \sin n\varphi) \tag{24}$$

- where

$$a_n = \frac{1}{\pi}\left\{ \int_0^{\Delta\varphi} V_1^2 \cos n\varphi d\varphi + \int_{\frac{\pi}{8}-\Delta\varphi}^{\frac{\pi}{8}+\Delta\varphi} V_2^2 \cos n\varphi d\varphi + \right.$$

$$\int_{\frac{\pi}{4}-\Delta\varphi}^{\frac{\pi}{4}+\Delta\varphi} V_3^2 \cos n\varphi d\varphi + \int_{\frac{3\pi}{8}-\Delta\varphi}^{\frac{3\pi}{8}+\Delta\varphi} V_4^2 \cos n\varphi d\varphi + \tag{25}$$

$$\int_{\frac{\pi}{2}-\Delta\varphi}^{\frac{\pi}{2}+\Delta\varphi} V_1^2 \cos n\varphi d\varphi + \int_{\frac{5\pi}{8}-\Delta\varphi}^{\frac{5\pi}{8}+\Delta\varphi} V_2^2 \cos n\varphi d\varphi + \tag{26}$$

$$\left. \cdots + \int_{2\pi-\Delta\varphi}^{2\pi} V_1^2 \cos n\varphi d\varphi \right\}, \quad n = 0, 1, 2 \cdots . \tag{27}$$

Fourier series for $V^2(\varphi)$

- 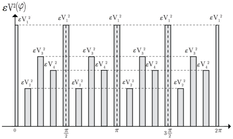

- $$V^2(\varphi) = \frac{a_0}{2} + \sum_{n=1}^{\infty} \left(a_n \cos n\varphi + b_n \sin n\varphi\right) \tag{24}$$

- where

$$a_n = \frac{1}{\pi}\left\{\int_0^{\Delta\varphi} V_1^2 \cos n\varphi d\varphi + \int_{\frac{\pi}{8}-\Delta\varphi}^{\frac{\pi}{8}+\Delta\varphi} V_2^2 \cos n\varphi d\varphi + \right.$$

$$\int_{\frac{\pi}{4}-\Delta\varphi}^{\frac{\pi}{4}+\Delta\varphi} V_3^2 \cos n\varphi d\varphi + \int_{\frac{3\pi}{8}-\Delta\varphi}^{\frac{3\pi}{8}+\Delta\varphi} V_4^2 \cos n\varphi d\varphi + \tag{25}$$

$$\int_{\frac{\pi}{2}-\Delta\varphi}^{\frac{\pi}{2}+\Delta\varphi} V_1^2 \cos n\varphi d\varphi + \int_{\frac{5\pi}{8}-\Delta\varphi}^{\frac{5\pi}{8}+\Delta\varphi} V_2^2 \cos n\varphi d\varphi + \tag{26}$$

$$\left. \cdots + \int_{2\pi-\Delta\varphi}^{2\pi} V_1^2 \cos n\varphi d\varphi \right\}, \quad n = 0, 1, 2 \cdots. \tag{27}$$

Fourier series for $V^2(\varphi)$

- The CAS MATHEMATICA® was used calculate the Fourier coefficient a_n. The code is indicated in the following figure

Fourier series for $V^2(\varphi)$

- The CAS MATHEMATICA® was used calculate the Fourier coefficient a_n. The code is indicated in the following figure

In[1]:= $a_{n\_}$:=

$$
\begin{aligned}
&\frac{1}{\pi}\,\text{FullSimplify}\Big[\int_0^{\Delta\varphi} V_1^2\,\text{Cos}[n\,\varphi]\,d\varphi + \int_{\frac{\pi}{8}-\Delta\varphi}^{\frac{\pi}{8}+\Delta\varphi} V_2^2\,\text{Cos}[n\,\varphi]\,d\varphi + \\
&\int_{\frac{\pi}{4}-\Delta\varphi}^{\frac{\pi}{4}+\Delta\varphi} V_3^2\,\text{Cos}[n\,\varphi]\,d\varphi + \int_{\frac{3\pi}{8}-\Delta\varphi}^{\frac{3\pi}{8}+\Delta\varphi} V_4^2\,\text{Cos}[n\,\varphi]\,d\varphi + \int_{\frac{\pi}{2}-\Delta\varphi}^{\frac{\pi}{2}+\Delta\varphi} V_1^2\,\text{Cos}[n\,\varphi]\,d\varphi + \\
&\int_{\frac{5\pi}{8}-\Delta\varphi}^{\frac{5\pi}{8}+\Delta\varphi} V_2^2\,\text{Cos}[n\,\varphi]\,d\varphi + \int_{\frac{3\pi}{4}-\Delta\varphi}^{\frac{3\pi}{4}+\Delta\varphi} V_3^2\,\text{Cos}[n\,\varphi]\,d\varphi + \int_{\frac{7\pi}{8}-\Delta\varphi}^{\frac{7\pi}{8}+\Delta\varphi} V_4^2\,\text{Cos}[n\,\varphi]\,d\varphi + \\
&\int_{\pi-\Delta\varphi}^{\pi+\Delta\varphi} V_1^2\,\text{Cos}[n\,\varphi]\,d\varphi + \int_{\frac{9\pi}{8}-\Delta\varphi}^{\frac{9\pi}{8}+\Delta\varphi} V_2^2\,\text{Cos}[n\,\varphi]\,d\varphi + \int_{\frac{5\pi}{4}-\Delta\varphi}^{\frac{5\pi}{4}+\Delta\varphi} V_3^2\,\text{Cos}[n\,\varphi]\,d\varphi + \\
&\int_{\frac{11\pi}{8}-\Delta\varphi}^{\frac{11\pi}{8}+\Delta\varphi} V_4^2\,\text{Cos}[n\,\varphi]\,d\varphi + \int_{\frac{3\pi}{2}-\Delta\varphi}^{\frac{3\pi}{2}+\Delta\varphi} V_1^2\,\text{Cos}[n\,\varphi]\,d\varphi + \int_{\frac{13\pi}{8}-\Delta\varphi}^{\frac{13\pi}{8}+\Delta\varphi} V_2^2\,\text{Cos}[n\,\varphi]\,d\varphi + \\
&\int_{\frac{7\pi}{4}-\Delta\varphi}^{\frac{7\pi}{4}+\Delta\varphi} V_3^2\,\text{Cos}[n\,\varphi]\,d\varphi + \int_{\frac{15\pi}{8}-\Delta\varphi}^{\frac{15\pi}{8}+\Delta\varphi} V_4^2\,\text{Cos}[n\,\varphi]\,d\varphi + \int_{2\pi-\Delta\varphi}^{2\pi} \left(V_1^2\,\text{Cos}[n\,\varphi]\right)d\varphi\Big]
\end{aligned}
$$

Table[a_n, {n, 0, 14}]

Out[2]=
$$
\Big\{\frac{8\,\Delta\varphi\,\left(V_1^2+V_2^2+V_3^2+V_4^2\right)}{\pi},\ 0,\ 0,\ 0,\ \frac{2\,\text{Sin}[4\,\Delta\varphi]\,\left(V_1^2-V_3^2\right)}{\pi},\ 0,\ 0,\ 0,\ \frac{\text{Sin}[8\,\Delta\varphi]\,\left(V_1^2-V_2^2+V_3^2-V_4^2\right)}{\pi},\ 0,\ 0,\ 0,\ \frac{2\,\text{Sin}[12\,\Delta\varphi]\,\left(V_1^2-V_3^2\right)}{3\,\pi},\ 0,\ 0\Big\}
$$

-

Fourier series for $V^2(\varphi)$

- A Figure of the code used to calculate the Fourier coefficient b_n follows:

Fourier series for $V^2(\varphi)$

- A Figure of the code used to calculate the Fourier coefficient b_n follows:

In[9]:= $\mathtt{b}_{n\_}$:=

$$
\begin{aligned}
&\frac{1}{\pi}\,\mathtt{FullSimplify}\Big[\int_0^{\Delta\varphi} V_1^2\,\mathtt{Sin}[n\,\varphi]\,d\varphi + \int_{\frac{\pi}{8}-\Delta\varphi}^{\frac{\pi}{8}+\Delta\varphi} V_2^2\,\mathtt{Sin}[n\,\varphi]\,d\varphi + \int_{\frac{\pi}{4}-\Delta\varphi}^{\frac{\pi}{4}+\Delta\varphi} V_3^2\,\mathtt{Sin}[n\,\varphi]\,d\varphi + \\
&\int_{\frac{3\pi}{8}-\Delta\varphi}^{\frac{3\pi}{8}+\Delta\varphi} V_4^2\,\mathtt{Sin}[n\,\varphi]\,d\varphi + \int_{\frac{\pi}{2}-\Delta\varphi}^{\frac{\pi}{2}+\Delta\varphi} V_1^2\,\mathtt{Sin}[n\,\varphi]\,d\varphi + \int_{\frac{5\pi}{8}-\Delta\varphi}^{\frac{5\pi}{8}+\Delta\varphi} V_2^2\,\mathtt{Sin}[n\,\varphi]\,d\varphi + \\
&\int_{\frac{3\pi}{4}-\Delta\varphi}^{\frac{3\pi}{4}+\Delta\varphi} V_3^2\,\mathtt{Sin}[n\,\varphi]\,d\varphi + \int_{\frac{7\pi}{8}-\Delta\varphi}^{\frac{7\pi}{8}+\Delta\varphi} V_4^2\,\mathtt{Sin}[n\,\varphi]\,d\varphi + \int_{\pi-\Delta\varphi}^{\pi+\Delta\varphi} V_1^2\,\mathtt{Sin}[n\,\varphi]\,d\varphi + \\
&\int_{\frac{9\pi}{8}-\Delta\varphi}^{\frac{9\pi}{8}+\Delta\varphi} V_2^2\,\mathtt{Sin}[n\,\varphi]\,d\varphi + \int_{\frac{5\pi}{4}-\Delta\varphi}^{\frac{5\pi}{4}+\Delta\varphi} V_3^2\,\mathtt{Sin}[n\,\varphi]\,d\varphi + \int_{\frac{11\pi}{8}-\Delta\varphi}^{\frac{11\pi}{8}+\Delta\varphi} V_4^2\,\mathtt{Sin}[n\,\varphi]\,d\varphi + \\
&\int_{\frac{3\pi}{2}-\Delta\varphi}^{\frac{3\pi}{2}+\Delta\varphi} V_1^2\,\mathtt{Sin}[n\,\varphi]\,d\varphi + \int_{\frac{13\pi}{8}-\Delta\varphi}^{\frac{13\pi}{8}+\Delta\varphi} V_2^2\,\mathtt{Sin}[n\,\varphi]\,d\varphi + \int_{\frac{7\pi}{4}-\Delta\varphi}^{\frac{7\pi}{4}+\Delta\varphi} V_3^2\,\mathtt{Sin}[n\,\varphi]\,d\varphi + \\
&\int_{\frac{15\pi}{8}-\Delta\varphi}^{\frac{15\pi}{8}+\Delta\varphi} V_4^2\,\mathtt{Sin}[n\,\varphi]\,d\varphi + \int_{2\pi-\Delta\varphi}^{2\pi} \left(V_1^2\,\mathtt{Sin}[n\,\varphi]\right)d\varphi\Big]
\end{aligned}
$$

```
Table[b_n, {n, 1, 14}]
```

- Out[10]= $\left\{0,\ 0,\ 0,\ \frac{2\,\mathtt{Sin}[4\,\Delta\varphi]\,\left(V_2^2 - V_4^2\right)}{\pi},\ 0,\ 0,\ 0,\ 0,\ 0,\ 0,\ 0,\ \frac{2\,\mathtt{Sin}[12\,\Delta\varphi]\,\left(-V_2^2 + V_4^2\right)}{3\,\pi},\ 0,\ 0\right\}$

Using orthogonality

- Vibratory gyroscopes usually work with the mode of vibration determined by the $m = 2$ circumferential wave number. The vibration pattern is illustrated in the following figure:

Using orthogonality

- Vibratory gyroscopes usually work with the mode of vibration determined by the $m = 2$ circumferential wave number. The vibration pattern is illustrated in the following figure:

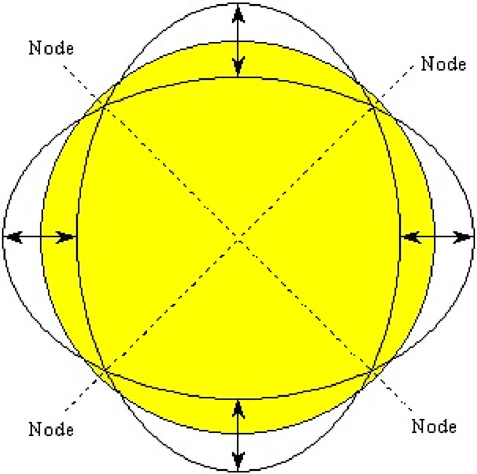

-

Using orthogonality continued

- Recall that for the circumferential wave number $m = 2$

$$u\left(q,\varphi,t\right) = U(q)\left[C\left(t\right)\cos 2\varphi + S\left(t\right)\sin 2\varphi\right]. \tag{28}$$

- The "TrigReduce" command in MATHEMATICA® yields u_q^2 reveals that:

$$u_q^2 = U^2(q)\left[\frac{C^2+S^2}{2} + \frac{C^2-S^2}{2}\cos 4\varphi + CS\sin 4\varphi\right]. \tag{29}$$

- Consequently, because of the *orthogonality* of the sine and cosine functions, when we substitute the Fourier series for $V\left(\varphi\right)$ into

$$E_e = \frac{\epsilon_0 hq}{2d}\int_0^{2\pi} \varepsilon V^2\left(\varphi\right)\left[1 + \frac{u_q}{d} + \frac{u_q^2}{d^2}\right] d\varphi, \tag{30}$$

only the zeroth harmonic and the 4^{th} harmonic are salient and we can neglect $\frac{u_q}{d}$.

Using orthogonality continued

- Recall that for the circumferential wave number $m = 2$

$$u\left(q,\varphi,t\right) = U(q)[C\left(t\right)\cos 2\varphi + S\left(t\right)\sin 2\varphi]. \tag{28}$$

- The "TrigReduce" command in MATHEMATICA® yields u_q^2 reveals that:

$$u_q^2 = U^2(q)[\frac{C^2+S^2}{2} + \frac{C^2-S^2}{2}\cos 4\varphi + CS\sin 4\varphi]. \tag{29}$$

- Consequently, because of the *orthogonality* of the sine and cosine functions, when we substitute the Fourier series for $V(\varphi)$ into

$$E_e = \frac{\epsilon_0 hq}{2d}\int_0^{2\pi} \varepsilon V^2(\varphi)\left[1 + \frac{u_q}{d} + \frac{u_q^2}{d^2}\right] d\varphi, \tag{30}$$

only the zeroth harmonic and the 4^{th} harmonic are salient and we can neglect $\frac{u_q}{d}$.

Using orthogonality continued

- Recall that for the circumferential wave number $m = 2$

$$u(q, \varphi, t) = U(q)[C(t)\cos 2\varphi + S(t)\sin 2\varphi]. \tag{28}$$

- The "TrigReduce" command in MATHEMATICA® yields u_q^2 reveals that:

$$u_q^2 = U^2(q)[\frac{C^2+S^2}{2} + \frac{C^2-S^2}{2}\cos 4\varphi + CS\sin 4\varphi]. \tag{29}$$

- Consequently, because of the *orthogonality* of the sine and cosine functions, when we substitute the Fourier series for $V(\varphi)$ into

$$E_e = \frac{\epsilon_0 hq}{2d}\int_0^{2\pi} \varepsilon V^2(\varphi)\left[1 + \frac{u_q}{d} + \frac{u_q^2}{d^2}\right] d\varphi, \tag{30}$$

only the zeroth harmonic and the 4^{th} harmonic are salient and we can neglect $\frac{u_q}{d}$.

Total electrical potential energy in terms of Fourier coefficients

- Hence, using the tables of Fourier coefficients generated by MATHEMATICA®,

$$E_e = \frac{\epsilon_0 hq}{2d} \int_0^{2\pi} \varepsilon \left\{ \frac{4\Delta\varphi \left(V_1^2 + V_2^2 + V_3^2 + V_4^2\right)}{\pi} + \right.$$

$$\frac{2\left(V_1^2 - V_3^2\right)\sin(4\Delta\varphi)}{\pi} \cos 4\varphi +$$

$$\left. \frac{2\left(V_2^2 - V_4^2\right)\sin(4\Delta\varphi)}{\pi} \sin 4\varphi \right\} \times$$

$$\left\{ 1 + \frac{u_q^2}{d^2} \right\} d\varphi \qquad (31)$$

Total electrical potential energy in terms of Fourier coefficients continued

- Using MATHEMATICA® to do the book-keeping, we find

$$E_e = \pi\varepsilon\left\{k_0 + \frac{1}{2}k_1\left(C^2 + S^2\right) + \frac{1}{2}k_2\left(C^2 - S^2\right) + k_3 CS\right\} \tag{32}$$

- where

$$k_0 = \frac{4\Delta\varphi h q \epsilon_0}{\pi d}\left(V_1^2 + V_2^2 + V_3^2 + V_4^2\right) \tag{33}$$

$$k_1 = \frac{4\Delta\varphi h q \epsilon_0 U^2(q)}{\pi d^3}\left(V_1^2 + V_2^2 + V_3^2 + V_4^2\right) \tag{34}$$

$$k_2 = \frac{h q \epsilon_0 \sin(4\Delta\varphi) U^2(q)}{\pi d^3}\left(V_1^2 - V_3^2\right) \tag{35}$$

$$k_3 = \frac{h q \epsilon_0 \sin(4\Delta\varphi) U^2(q)}{\pi d^3}\left(V_2^2 - V_4^2\right) \tag{36}$$

Total electrical potential energy in terms of Fourier coefficients continued

- Using MATHEMATICA® to do the book-keeping, we find

$$E_e = \pi\varepsilon \left\{ k_0 + \frac{1}{2}k_1 \left(C^2 + S^2\right) + \frac{1}{2}k_2\left(C^2 - S^2\right) + k_3\, CS \right\} \tag{32}$$

- where

$$k_0 = \frac{4\Delta\varphi hq\epsilon_0}{\pi d}\left(V_1^2 + V_2^2 + V_3^2 + V_4^2\right) \tag{33}$$

$$k_1 = \frac{4\Delta\varphi hq\epsilon_0\, U^2(q)}{\pi d^3}\left(V_1^2 + V_2^2 + V_3^2 + V_4^2\right) \tag{34}$$

$$k_2 = \frac{hq\epsilon_0 \sin(4\Delta\varphi)\, U^2(q)}{\pi d^3}\left(V_1^2 - V_3^2\right) \tag{35}$$

$$k_3 = \frac{hq\epsilon_0 \sin(4\Delta\varphi)\, U^2(q)}{\pi d^3}\left(V_2^2 - V_4^2\right) \tag{36}$$

Equations of motion including the capacitors

- We include the electrical potential energy into the Lagrangian L as follows

$$L = E_k - E_p + E_e$$

- Hence

$$\begin{aligned} L = {} & \tfrac{\pi}{2} I_0(\dot{C}^2 + \dot{S}^2) + \\ & \varepsilon\pi \left[I_1\Omega(\dot{C}S - C\dot{S}) + \tfrac{\pi}{2} I_0\rho_c(\dot{C}^2 - \dot{S}^2) + \pi I_0\rho_s \dot{C}\dot{S} \right] - \\ & \tfrac{\pi}{2} I_2 \left(C^2 + S^2 \right) + \varepsilon\pi \left[k_0 + \tfrac{1}{2} k_1 \left(C^2 + S^2 \right) + \tfrac{1}{2} k_2 (C^2 - S^2) + k_3 CS \right]. \end{aligned} \tag{37}$$

- The two applicable Euler-Lagrange Equations of motion are

$$\frac{d}{dt}\left(\frac{\partial L}{\partial \dot{C}}\right) - \left(\frac{\partial L}{\partial C}\right) = 0 \quad \& \quad \frac{d}{dt}\left(\frac{\partial L}{\partial \dot{S}}\right) - \left(\frac{\partial L}{\partial S}\right) = 0 \tag{38}$$

Equations of motion including the capacitors

- We include the electrical potential energy into the Lagrangian L as follows

$$L = E_k - E_p + E_e$$

- Hence

$$L = \frac{\pi}{2} I_0 (\dot{C}^2 + \dot{S}^2) + \varepsilon\pi \left[I_1 \Omega (\dot{C}S - C\dot{S}) + \frac{\pi}{2} I_0 \rho_c (\dot{C}^2 - \dot{S}^2) + \pi I_0 \rho_s \dot{C}\dot{S} \right] - \frac{\pi}{2} I_2 \left(C^2 + S^2 \right) + \varepsilon\pi \left[k_0 + \frac{1}{2} k_1 \left(C^2 + S^2 \right) + \frac{1}{2} k_2 (C^2 - S^2) + k_3 CS \right]. \tag{37}$$

- The two applicable Euler-Lagrange Equations of motion are

$$\frac{d}{dt}\left(\frac{\partial L}{\partial \dot{C}}\right) - \left(\frac{\partial L}{\partial C}\right) = 0 \quad \& \quad \frac{d}{dt}\left(\frac{\partial L}{\partial \dot{S}}\right) - \left(\frac{\partial L}{\partial S}\right) = 0 \tag{38}$$

Equations of motion including the capacitors

- We include the electrical potential energy into the Lagrangian L as follows

$$L = E_k - E_p + E_e$$

- Hence

$$L = \tfrac{\pi}{2} I_0 (\dot{C}^2 + \dot{S}^2) + \varepsilon\pi \left[I_1 \Omega (\dot{C} S - C \dot{S}) + \tfrac{\pi}{2} I_0 \rho_c (\dot{C}^2 - \dot{S}^2) + \pi I_0 \rho_s \dot{C} \dot{S} \right] - \tfrac{\pi}{2} I_2 \left(C^2 + S^2 \right) + \varepsilon\pi \left[k_0 + \tfrac{1}{2} k_1 \left(C^2 + S^2 \right) + \tfrac{1}{2} k_2 (C^2 - S^2) + k_3 CS \right]. \tag{37}$$

- The two applicable Euler-Lagrange Equations of motion are

$$\frac{d}{dt}\left(\frac{\partial L}{\partial \dot{C}}\right) - \left(\frac{\partial L}{\partial C}\right) = 0 \quad \& \quad \frac{d}{dt}\left(\frac{\partial L}{\partial \dot{S}}\right) - \left(\frac{\partial L}{\partial S}\right) = 0 \tag{38}$$

Equations of motion including the capacitors continued

- A figure showing some of the MATHEMATICA® code used to calculate the equations of motion follows

Equations of motion including the capacitors continued

- A figure showing some of the MATHEMATICA® code used to calculate the equations of motion follows

In[94]:= $\mathbf{L} = \mathbb{E}_k - \mathbb{E}_p + \mathbb{E}_e$

Out[94]=

$$\pi \in k_0 + \frac{1}{2} \pi \in \left(C[t]^2 + S[t]^2\right) k_1 + \frac{1}{2} \pi \in \left(C[t]^2 - S[t]^2\right) k_2 + \pi C[t]\, S[t]\, k_3 - \mathbb{E}_p + \frac{1}{2} \pi \mathbb{I}_0 \left(C'[t]^2 + S'[t]^2\right) + \pi \in \left(\Omega\, \mathbb{I}_1 \left(S[t]\, C'[t] - C[t]\, S'[t]\right) + \frac{1}{2} \mathbb{I}_0 \left(2 \rho_s C'[t]\, S'[t] + \rho_c \left(C'[t]^2 - S'[t]^2\right)\right)\right)$$

In[95]:= $\mathbf{Eq1} = \mathbf{Expand}\left[\frac{\partial_t\, \partial_{C'[t]} \mathbf{L} - \partial_{C[t]} \mathbf{L}}{\pi\, \mathbb{I}_0} == 0\right] /. \left\{\frac{\mathbb{I}_1}{\mathbb{I}_0} \to \eta\right\}$

Out[95]=

$$-\frac{\in C[t]\, k_1}{\mathbb{I}_0} - \frac{\in C[t]\, k_2}{\mathbb{I}_0} - \frac{S[t]\, k_3}{\mathbb{I}_0} + 2 \in \eta\, \Omega\, S'[t] + C''[t] + \in \rho_c C''[t] + \in \rho_s S''[t] == 0$$

-

Equations of motion including the capacitors continued

- Neglecting terms of $O(\varepsilon^2)$, the equations of motion produced by MATHEMATICA® can be written in matrix form as follows:

-
$$\begin{pmatrix} 1+\varepsilon\rho_c & \varepsilon\rho_s \\ \varepsilon\rho_s & 1-\varepsilon\rho_c \end{pmatrix} \begin{pmatrix} \ddot{C} \\ \ddot{S} \end{pmatrix} + \frac{1}{I_0} \begin{pmatrix} I_2-\varepsilon k_1-\varepsilon k_2 & -\varepsilon k_3 \\ -\varepsilon k_3 & I_2-\varepsilon k_1+\varepsilon I_2 \end{pmatrix} \begin{pmatrix} C \\ S \end{pmatrix} - 2\eta\varepsilon\Omega \begin{pmatrix} 0 & -1 \\ 1 & 0 \end{pmatrix} \begin{pmatrix} \dot{C} \\ \dot{S} \end{pmatrix} = 0 \quad (39)$$

- The inverse matrix of the leading coefficent matrix is:

-
$$\begin{pmatrix} 1-\varepsilon\rho_c & -\varepsilon\rho_s \\ -\varepsilon\rho_s & 1+\varepsilon\rho_c \end{pmatrix}$$

Equations of motion including the capacitors continued

- Neglecting terms of $O(\varepsilon^2)$, the equations of motion produced by MATHEMATICA® can be written in matrix form as follows:
-
$$\begin{pmatrix} 1+\varepsilon\rho_c & \varepsilon\rho_s \\ \varepsilon\rho_s & 1-\varepsilon\rho_c \end{pmatrix} \begin{pmatrix} \ddot{C} \\ \ddot{S} \end{pmatrix} + \frac{1}{l_0} \begin{pmatrix} l_2-\varepsilon k_1-\varepsilon k_2 & -\varepsilon k_3 \\ -\varepsilon k_3 & l_2-\varepsilon k_1+\varepsilon l_2 \end{pmatrix} \begin{pmatrix} C \\ S \end{pmatrix} - 2\eta\varepsilon\Omega \begin{pmatrix} 0 & -1 \\ 1 & 0 \end{pmatrix} \begin{pmatrix} \dot{C} \\ \dot{S} \end{pmatrix} = 0 \tag{39}$$
- The inverse matrix of the leading coefficent matrix is:
-
$$\begin{pmatrix} 1-\varepsilon\rho_c & -\varepsilon\rho_s \\ -\varepsilon\rho_s & 1+\varepsilon\rho_c \end{pmatrix}$$

Equations of motion including the capacitors continued

- Neglecting terms of $O(\varepsilon^2)$, the equations of motion produced by MATHEMATICA® can be written in matrix form as follows:
- $$\begin{pmatrix} 1+\varepsilon\rho_c & \varepsilon\rho_s \\ \varepsilon\rho_s & 1-\varepsilon\rho_c \end{pmatrix} \begin{pmatrix} \ddot{C} \\ \ddot{S} \end{pmatrix} + \frac{1}{I_0} \begin{pmatrix} I_2-\varepsilon k_1-\varepsilon k_2 & -\varepsilon k_3 \\ -\varepsilon k_3 & I_2-\varepsilon k_1+\varepsilon I_2 \end{pmatrix} \begin{pmatrix} C \\ S \end{pmatrix} - 2\eta\varepsilon\Omega \begin{pmatrix} 0 & -1 \\ 1 & 0 \end{pmatrix} \begin{pmatrix} \dot{C} \\ \dot{S} \end{pmatrix} = 0 \quad (39)$$
- The inverse matrix of the leading coefficent matrix is:
- $$\begin{pmatrix} 1-\varepsilon\rho_c & -\varepsilon\rho_s \\ -\varepsilon\rho_s & 1+\varepsilon\rho_c \end{pmatrix}$$

Equations of motion including the capacitors continued

- Neglecting terms of $O(\varepsilon^2)$, the equations of motion produced by MATHEMATICA® can be written in matrix form as follows:

- $$\begin{pmatrix} 1+\varepsilon\rho_c & \varepsilon\rho_s \\ \varepsilon\rho_s & 1-\varepsilon\rho_c \end{pmatrix} \begin{pmatrix} \ddot{C} \\ \ddot{S} \end{pmatrix} + \frac{1}{l_0} \begin{pmatrix} l_2-\varepsilon k_1-\varepsilon k_2 & -\varepsilon k_3 \\ -\varepsilon k_3 & l_2-\varepsilon k_1+\varepsilon l_2 \end{pmatrix} \begin{pmatrix} C \\ S \end{pmatrix} - 2\eta\varepsilon\Omega \begin{pmatrix} 0 & -1 \\ 1 & 0 \end{pmatrix} \begin{pmatrix} \dot{C} \\ \dot{S} \end{pmatrix} = 0 \quad (39)$$

- The inverse matrix of the leading coefficent matrix is:

- $$\begin{pmatrix} 1-\varepsilon\rho_c & -\varepsilon\rho_s \\ -\varepsilon\rho_s & 1+\varepsilon\rho_c \end{pmatrix}$$

Equations of motion including the capacitors continued

- Multiplying the matrix equation

$$\begin{pmatrix} 1+\varepsilon\rho_c & \varepsilon\rho_s \\ \varepsilon\rho_s & 1-\varepsilon\rho_c \end{pmatrix} \begin{pmatrix} \ddot{C} \\ \ddot{S} \end{pmatrix} + \frac{1}{l_0} \begin{pmatrix} l_2 - \varepsilon k_1 - \varepsilon k_2 & -\varepsilon k_3 \\ -\varepsilon k_3 & l_2 - \varepsilon k_1 + \varepsilon l_2 \end{pmatrix} \begin{pmatrix} C \\ S \end{pmatrix} = 2\eta\varepsilon\Omega \begin{pmatrix} 0 & -1 \\ 1 & 0 \end{pmatrix} \begin{pmatrix} \dot{C} \\ \dot{S} \end{pmatrix} \tag{40}$$

  through by this inverse matrix yields (neglecting $O(\varepsilon^2)$) yields:

-

$$\begin{pmatrix} \ddot{C} \\ \ddot{S} \end{pmatrix} + \frac{1}{l_0} \begin{pmatrix} l_2 - \varepsilon\left(k_1 + k_2 + \rho_c l_2\right) & -\varepsilon\left(k_3 + \rho_s l_2\right) \\ -\varepsilon\left(k_3 + \rho_s l_2\right) & l_2 + \varepsilon\left(-k_1 + k_2 + \rho_c l_2\right) \end{pmatrix} \begin{pmatrix} C \\ S \end{pmatrix} = 2\eta\varepsilon\Omega \begin{pmatrix} 0 & -1 \\ 1 & 0 \end{pmatrix} \begin{pmatrix} \dot{C} \\ \dot{S} \end{pmatrix} \tag{41}$$

Equations of motion including the capacitors continued

- Multiplying the matrix equation

$$\begin{pmatrix} 1+\varepsilon\rho_c & \varepsilon\rho_s \\ \varepsilon\rho_s & 1-\varepsilon\rho_c \end{pmatrix} \begin{pmatrix} \ddot{C} \\ \ddot{S} \end{pmatrix} + \frac{1}{l_0} \begin{pmatrix} l_2-\varepsilon k_1-\varepsilon k_2 & -\varepsilon k_3 \\ -\varepsilon k_3 & l_2-\varepsilon k_1+\varepsilon l_2 \end{pmatrix} \begin{pmatrix} C \\ S \end{pmatrix} = 2\eta\varepsilon\Omega \begin{pmatrix} 0 & -1 \\ 1 & 0 \end{pmatrix} \begin{pmatrix} \dot{C} \\ \dot{S} \end{pmatrix} \tag{40}$$

through by this inverse matrix yields (neglecting $O(\varepsilon^2)$) yields:

-

$$\begin{pmatrix} \ddot{C} \\ \ddot{S} \end{pmatrix} + \frac{1}{l_0} \begin{pmatrix} l_2-\varepsilon\left(k_1+k_2+\rho_c l_2\right) & -\varepsilon\left(k_3+\rho_s l_2\right) \\ -\varepsilon\left(k_3+\rho_s l_2\right) & l_2+\varepsilon\left(-k_1+k_2+\rho_c l_2\right) \end{pmatrix} \begin{pmatrix} C \\ S \end{pmatrix} = 2\eta\varepsilon\Omega \begin{pmatrix} 0 & -1 \\ 1 & 0 \end{pmatrix} \begin{pmatrix} \dot{C} \\ \dot{S} \end{pmatrix} \tag{41}$$

Controlling mass imperfections

- Examining the equations of motion that include mass imperfections:

$$
\begin{pmatrix} \ddot{C} \\ \ddot{S} \end{pmatrix} + \frac{1}{I_0} \begin{pmatrix} I_2 - \varepsilon k_1 - \varepsilon \left[k_2 + \rho_c I_2 \right] & -\varepsilon \left[k_3 + \rho_s I_2 \right] \\ -\varepsilon \left[k_3 + \rho_s I_2 \right] & I_2 - \varepsilon k_1 + \varepsilon \left[k_2 + \rho_c I_2 \right] \end{pmatrix} \begin{pmatrix} C \\ S \end{pmatrix} = 2\eta\varepsilon\Omega \begin{pmatrix} 0 & -1 \\ 1 & 0 \end{pmatrix} \begin{pmatrix} \dot{C} \\ \dot{S} \end{pmatrix}, \tag{42}
$$

- if we arrange capacitor voltage so that

$$
\varepsilon \left[k_2 + \rho_c I_2 \right] = 0 \quad \& \quad \varepsilon \left[k_2 + \rho_c I_2 \right] = 0
$$

then the equations of motion reduce to

$$
\begin{pmatrix} \ddot{C} \\ \ddot{S} \end{pmatrix} + \frac{I_2 - \varepsilon k_1}{I_0} \begin{pmatrix} C \\ S \end{pmatrix} = 2\eta\varepsilon\Omega \begin{pmatrix} 0 & -1 \\ 1 & 0 \end{pmatrix} \begin{pmatrix} \dot{C} \\ \dot{S} \end{pmatrix}. \tag{43}
$$

Controlling mass imperfections

- Examining the equations of motion that include mass imperfections:

$$\begin{pmatrix} \ddot{C} \\ \ddot{S} \end{pmatrix} + \frac{1}{I_0} \begin{pmatrix} I_2 - \varepsilon k_1 - \varepsilon\left[k_2 + \rho_c I_2\right] & -\varepsilon\left[k_3 + \rho_s I_2\right] \\ -\varepsilon\left[k_3 + \rho_s I_2\right] & I_2 - \varepsilon k_1 + \varepsilon\left[k_2 + \rho_c I_2\right] \end{pmatrix} \begin{pmatrix} C \\ S \end{pmatrix}$$
$$= 2\eta\varepsilon\Omega \begin{pmatrix} 0 & -1 \\ 1 & 0 \end{pmatrix} \begin{pmatrix} \dot{C} \\ \dot{S} \end{pmatrix}, \qquad (42)$$

- if we arrange capacitor voltage so that

$$\varepsilon\left[k_2 + \rho_c I_2\right] = 0 \quad \& \quad \varepsilon\left[k_2 + \rho_c I_2\right] = 0$$

then the equations of motion reduce to

$$\begin{pmatrix} \ddot{C} \\ \ddot{S} \end{pmatrix} + \frac{I_2 - \varepsilon k_1}{I_0} \begin{pmatrix} C \\ S \end{pmatrix} = 2\eta\varepsilon\Omega \begin{pmatrix} 0 & -1 \\ 1 & 0 \end{pmatrix} \begin{pmatrix} \dot{C} \\ \dot{S} \end{pmatrix}. \qquad (43)$$

Negative stiffness

- It is possible to achieve

$$\varepsilon\left[k_2+\rho_c l_2\right]=0 \quad \& \quad \varepsilon\left[k_2+\rho_c l_2\right]=0,$$

- that is, it is possible to achieve

$$k_2=-\rho_c l_2 \quad \& \quad k_3=-\rho_s l_2$$

because we may manipulate capacitors changing the size and sign of k_1 and k_2 since

$$k_2 \propto \left(V_1^2-V_3^2\right) \quad \& \quad k_3 \propto \left(V_2^2-V_4^2\right).$$

- Consider that the equations of motion of an *ideal cylindrical ring gyroscope* are

$$\begin{pmatrix}\ddot{C}\\ \ddot{S}\end{pmatrix}+\frac{l_2}{l_0}\begin{pmatrix}C\\ S\end{pmatrix}=2\eta\varepsilon\Omega\begin{pmatrix}0 & -1\\ 1 & 0\end{pmatrix}\begin{pmatrix}\dot{C}\\ \dot{S}\end{pmatrix} \tag{44}$$

while those of a *cylindrical ring gyroscope with mass imperfections* and a capacitor array set appropriately are:

$$\begin{pmatrix}\ddot{C}\\ \ddot{S}\end{pmatrix}+\frac{l_2-\varepsilon k_1}{l_0}\begin{pmatrix}C\\ S\end{pmatrix}=2\eta\varepsilon\Omega\begin{pmatrix}0 & -1\\ 1 & 0\end{pmatrix}\begin{pmatrix}\dot{C}\\ \dot{S}\end{pmatrix}. \tag{45}$$

Negative stiffness

- It is possible to achieve

$$\varepsilon\left[k_2+\rho_c I_2\right]=0 \quad \& \quad \varepsilon\left[k_2+\rho_c I_2\right]=0,$$

- that is, it is possible to achieve

$$k_2=-\rho_c I_2 \quad \& \quad k_3=-\rho_s I_2$$

because we may manipulate capacitors changing the size and sign of k_1 and k_2 since

$$k_2 \propto \left(V_1^2-V_3^2\right) \quad \& \quad k_3 \propto \left(V_2^2-V_4^2\right).$$

- Consider that the equations of motion of an *ideal cylindrical ring gyroscope* are

$$\begin{pmatrix}\ddot{C}\\ \ddot{S}\end{pmatrix}+\frac{I_2}{I_0}\begin{pmatrix}C\\ S\end{pmatrix}=2\eta\varepsilon\Omega\begin{pmatrix}0 & -1\\ 1 & 0\end{pmatrix}\begin{pmatrix}\dot{C}\\ \dot{S}\end{pmatrix} \tag{44}$$

while those of a *cylindrical ring gyroscope with mass imperfections* and a capacitor array set appropriately are:

$$\begin{pmatrix}\ddot{C}\\ \ddot{S}\end{pmatrix}+\frac{I_2-\varepsilon k_1}{I_0}\begin{pmatrix}C\\ S\end{pmatrix}=2\eta\varepsilon\Omega\begin{pmatrix}0 & -1\\ 1 & 0\end{pmatrix}\begin{pmatrix}\dot{C}\\ \dot{S}\end{pmatrix}. \tag{45}$$

Negative stiffness

- It is possible to achieve

$$\varepsilon\left[k_2 + \rho_c I_2\right] = 0 \quad \& \quad \varepsilon\left[k_2 + \rho_c I_2\right] = 0,$$

- that is, it is possible to achieve

$$k_2 = -\rho_c I_2 \quad \& \quad k_3 = -\rho_s I_2$$

because we may manipulate capacitors changing the size and sign of k_1 and k_2 since

$$k_2 \propto \left(V_1^2 - V_3^2\right) \quad \& \quad k_3 \propto \left(V_2^2 - V_4^2\right).$$

- Consider that the equations of motion of an *ideal cylindrical ring gyroscope* are

$$\begin{pmatrix} \ddot{C} \\ \ddot{S} \end{pmatrix} + \frac{I_2}{I_0}\begin{pmatrix} C \\ S \end{pmatrix} = 2\eta\varepsilon\Omega \begin{pmatrix} 0 & -1 \\ 1 & 0 \end{pmatrix}\begin{pmatrix} \dot{C} \\ \dot{S} \end{pmatrix} \tag{44}$$

while those of a *cylindrical ring gyroscope with mass imperfections* and a capacitor array set appropriately are:

$$\begin{pmatrix} \ddot{C} \\ \ddot{S} \end{pmatrix} + \frac{I_2 - \varepsilon k_1}{I_0}\begin{pmatrix} C \\ S \end{pmatrix} = 2\eta\varepsilon\Omega \begin{pmatrix} 0 & -1 \\ 1 & 0 \end{pmatrix}\begin{pmatrix} \dot{C} \\ \dot{S} \end{pmatrix}. \tag{45}$$

Negative stiffness continued

- Consequently the equations of motion of an *ideal cylindrical ring gyroscope* may be written as:

$$\begin{pmatrix} \ddot{C} \\ \ddot{S} \end{pmatrix} + \omega^2 \begin{pmatrix} C \\ S \end{pmatrix} = 2\eta\varepsilon\Omega \begin{pmatrix} 0 & -1 \\ 1 & 0 \end{pmatrix} \begin{pmatrix} \dot{C} \\ \dot{S} \end{pmatrix} \tag{46}$$

  while those of a *cylindrical ring gyroscope with mass imperfections* may be written as:

$$\begin{pmatrix} \ddot{C} \\ \ddot{S} \end{pmatrix} + (\omega^*)^2 \begin{pmatrix} C \\ S \end{pmatrix} = 2\eta\varepsilon\Omega \begin{pmatrix} 0 & -1 \\ 1 & 0 \end{pmatrix} \begin{pmatrix} \dot{C} \\ \dot{S} \end{pmatrix}. \tag{47}$$

- Hence, the capacitors have produced a gyroscope with mass imperfections that behaves "ideally" and is vibrating with a reduced angular rate

$$\omega^* = \sqrt{\frac{I_2 - \varepsilon k_1}{I_0}} \quad k_1 \propto \left(V_1^2 + V_2^2 + V_3^2 + V_4^2\right)$$

  as opposed to the ideal angular rate of vibration

$$\omega = \sqrt{\frac{I_2}{I_0}}.$$

Negative stiffness continued

- Consequently the equations of motion of an *ideal cylindrical ring gyroscope* may be written as:

$$\begin{pmatrix} \ddot{C} \\ \ddot{S} \end{pmatrix} + \omega^2 \begin{pmatrix} C \\ S \end{pmatrix} = 2\eta\varepsilon\Omega \begin{pmatrix} 0 & -1 \\ 1 & 0 \end{pmatrix} \begin{pmatrix} \dot{C} \\ \dot{S} \end{pmatrix} \tag{46}$$

while those of a *cylindrical ring gyroscope with mass imperfections* may be written as:

$$\begin{pmatrix} \ddot{C} \\ \ddot{S} \end{pmatrix} + (\omega^*)^2 \begin{pmatrix} C \\ S \end{pmatrix} = 2\eta\varepsilon\Omega \begin{pmatrix} 0 & -1 \\ 1 & 0 \end{pmatrix} \begin{pmatrix} \dot{C} \\ \dot{S} \end{pmatrix}. \tag{47}$$

- Hence, the capacitors have produced a gyroscope with mass imperfections that behaves "ideally" and is vibrating with a reduced angular rate

$$\omega^* = \sqrt{\frac{I_2 - \varepsilon k_1}{I_0}} \quad k_1 \propto \left(V_1^2 + V_2^2 + V_3^2 + V_4^2\right)$$

as opposed to the ideal angular rate of vibration

$$\omega = \sqrt{\frac{I_2}{I_0}}.$$

Negative stiffness continued

- The term

$$k_1 = \frac{4\Delta\varphi hq\epsilon_0 U^2(q)}{\pi d^3}\left(V_1^2 + V_2^2 + V_3^2 + V_4^2\right)$$

is clearly positive. Consequently, the positive term εk_1 in

$$\omega^* = \sqrt{\frac{I_2 - \varepsilon k_1}{I_0}}$$

reduces the stiffness integral I_2 and is known as *negative stifness*.

- A cylindrical ring gyroscope manufactured by including this array of capacitors and manipulating them appropriately will be able to utilise Bryan's factor η to determine the rotation rate $\varepsilon\Omega$ of the vehicle in which it is mounted using the fomula

$$\varepsilon\Omega = \frac{\text{Rate of rotation of the vibrating pattern of the gyroscope}}{\eta}. \tag{48}$$

- The term

$$k_1 = \frac{4\Delta\varphi hq\epsilon_0 U^2(q)}{\pi d^3}\left(V_1^2 + V_2^2 + V_3^2 + V_4^2\right)$$

is clearly positive. Consequently, the positive term εk_1 in

$$\omega^* = \sqrt{\frac{I_2 - \varepsilon k_1}{I_0}}$$

reduces the stiffness integral I_2 and is known as *negative stifness*.

- A cylindrical ring gyroscope manufactured by including this array of capacitors and manipulating them appropriately will be able to utilise Bryan's factor η to determine the rotation rate $\varepsilon\Omega$ of the vehicle in which it is mounted using the fomula

$$\varepsilon\Omega = \frac{\text{Rate of rotation of the vibrating pattern of the gyroscope}}{\eta}. \tag{48}$$